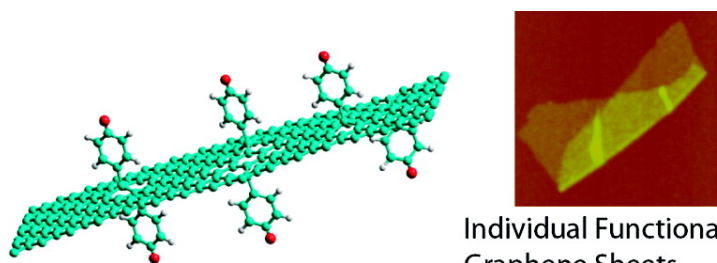


## Diazonium Functionalization of Surfactant-Wrapped Chemically Converted Graphene Sheets

Jay R. Lomeda, Condell D. Doyle, Dmitry V. Kosynkin, Wen-Fang Hwang, and James M. Tour

*J. Am. Chem. Soc.*, **2008**, 130 (48), 16201-16206 • DOI: 10.1021/ja806499w • Publication Date (Web): 08 November 2008

Downloaded from <http://pubs.acs.org> on February 8, 2009



Individual Functionalized Graphene Sheets

### More About This Article

Additional resources and features associated with this article are available within the HTML version:

- Supporting Information
- Access to high resolution figures
- Links to articles and content related to this article
- Copyright permission to reproduce figures and/or text from this article

[View the Full Text HTML](#)

## Diazonium Functionalization of Surfactant-Wrapped Chemically Converted Graphene Sheets

Jay R. Lomeda, Condell D. Doyle, Dmitry V. Kosynkin, Wen-Fang Hwang, and James M. Tour\*

Departments of Chemistry and Mechanical Engineering and Materials Science and the Smalley Institute for Nanoscale Science and Technology, Rice University, MS 222, 6100 Main Street, Houston, Texas 77005

Received January 17, 2008; E-mail: tour@rice.edu

**Abstract:** Surfactant-wrapped chemically converted graphene sheets obtained from reduction of graphene oxide with hydrazine were functionalized by treatment with aryl diazonium salts. The nanosheets are characterized by X-ray photoelectron spectroscopy, attenuated total reflectance infrared spectroscopy, Raman spectroscopy, atomic force microscopy, and transmission electron microscopy. The resulting functionalized nanosheets disperse readily in polar aprotic solvents, allowing alternative avenues for simple incorporation into different polymer matrices.

### Introduction

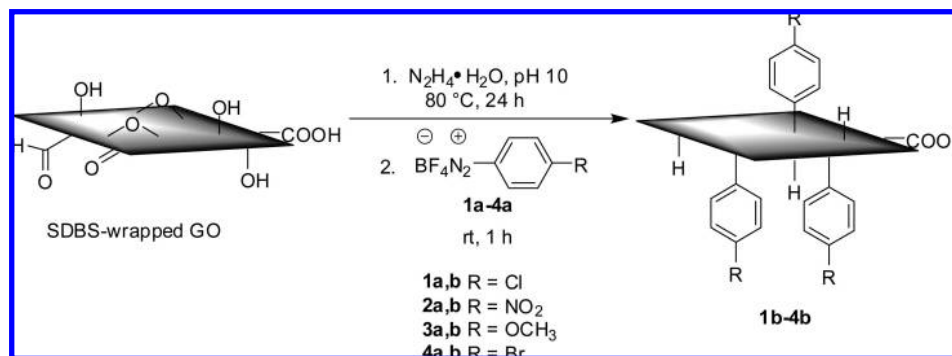
Oxidation of graphite to graphene oxide<sup>1</sup> (GO) allows for a high-yielding route to exfoliated carbon nanosheets.<sup>2</sup> The GO sheets disperse readily in water due to the presence of hydrophilic oxygen groups on the basal planes and edges,<sup>3</sup> although there may be variations depending on which oxidation method is used.<sup>4</sup> While the graphitic nature of the resulting nanosheets is highly compromised by oxidation, leading to loss of conductivity, reduction by chemical,<sup>2b,5</sup> thermal,<sup>6</sup> or electrochemical<sup>7</sup> treatment results in partial recovery of the graphitic character. The reduction step, while capable of removing a majority of the oxygen functionality, is still disordered when

compared to graphene, and hence, the product has been referred to as chemically converted graphene (CCG).<sup>8</sup> Nevertheless, the  $sp^2$  network is reestablished to a certain extent, as evidenced by the conductivity of the films when these nanosheets are deposited on different substrates,<sup>9</sup> powder X-ray diffraction,<sup>5b</sup> and the electron diffraction pattern.<sup>2a</sup>

While the “scotch tape” method<sup>10</sup> of removing thin sheets is convenient for trace amounts of material, the chemical exfoliation route using thermal expansion of graphite intercalation compounds (GIC)<sup>11</sup> is appealing to prepare materials for systems such as composites that require bulk quantities of graphene structures.<sup>12</sup> Functionalized graphene sheets obtained from rapid thermal expansion of GO have been shown to yield individual sheets that disperse readily in a variety of solvents.<sup>6a</sup> Furthermore, derivatization of the GO via the oxygen groups<sup>2b,5b,13,14</sup> has rendered the initial hydrophilic sheets hydrophobic. Preparation of CCG composites with minimal aggregation of the additive by in situ reduction of GO and its functionalized counterparts in different matrices has also been reported.<sup>12a,15</sup>

- (1) (a) Hummers, W. S.; Offeman, R. E. *J. Am. Chem. Soc.* **1958**, *80*, 1339. (b) Staudenmaier, L. *Ber. Dtsch. Chem. Ges.* **1898**, *31*, 1481–1489. (c) Brodie, B. *Ann. Chim. Phys.* **1855**, *45*, 351.
- (2) (a) Stankovich, S.; Dikin, D. A.; Dommett, G. H. B.; Kohlhaas, K. M.; Zimney, E. J.; Stach, E. A.; Piner, R. D.; Nguyen, S. T.; Ruoff, R. S. *Nature* **2006**, *442*, 282–286. (b) Stankovich, S.; Dikin, D. A.; Piner, R. D.; Kohlhaas, K. A.; Kleinhammes, A.; Jia, Y.; Wu, Y.; Nguyen, S. T.; Ruoff, R. S. *Carbon* **2007**, *4*, 1558–1565.
- (3) (a) Boehm, H. P.; Diehl, E.; Heck, W.; Sappok, R. *Angew. Chem.* **1964**, *76*, 742–751. (b) Kohlschutter, V.; Haenni, P. Z. *Anorg. Allg. Chem.* **1919**, *105*, 121–144. (c) Szabo, T.; Berkesi, O.; Forgo, P.; Josepovits, K.; Sanakis, Y.; Petridis, D.; Dekany, I. *Chem. Mater.* **2006**, *18*, 2740–2749. (d) Lerf, A.; He, H.; Forster, M.; Klinowski, J. *J. Phys. Chem. B* **1998**, *102*, 4477–4482. (e) He, H.; Klinowski, J.; Forster, M.; Lerf, A. *Chem. Phys. Lett.* **1998**, *287*, 53–56. (f) Mermoux, M.; Chabre, Y.; Rousseau, A. *Carbon* **1991**, *29*, 469–474. (g) Hontoria-Lucas, C.; López-Peinado, A. J.; López-González, J. de D.; Rojas-Cervantes, M. L.; Martín-Aranda, R. M. *Carbon* **1995**, *33*, 1585–1592.
- (4) Boehm, H. P.; Scholz, W. *Justus Liebigs Ann. Chem.* **1965**, *691*, 1–4.
- (5) (a) Stankovich, S.; Piner, R. D.; Chen, X. Q.; Wu, N. Q.; Nguyen, S. T.; Ruoff, R. S. *J. Mater. Chem.* **2006**, *16*, 155. (b) Bourlinos, A. B.; Gournis, D.; Petridis, D.; Szabo, T.; Szeri, A.; Dekany, I. *Langmuir* **2003**, *19*, 6050–6055.
- (6) (a) McAllister, M. J.; Li, J.-L.; Adamson, D. H.; Schniepp, H. C.; Abdala, A.; Liu, J.; Herrera-Alonso, M.; Milius, D. L.; Car, R.; Prud'homme, R. K.; Aksay, I. A. *Chem. Mater.* **2007**, *19*, 4396–4404. (b) Schniepp, H. C.; Li, J. L.; McAllister, M. J.; Sai, H.; Herrera-Alonso, M.; Adamson, D. H.; Prud'homme, R. K.; Car, R.; Saville, D. A.; Aksay, I. A. *J. Phys. Chem. B* **2006**, *110*, 8535–8539.
- (7) Voloshin, A. G.; Kolesnikova, I. P. *Elektrokhimiya* **1980**, *16*, 270.
- (8) Li, D.; Mueller, M. B.; Gilje, S.; Kaner, R. B.; Wallace, G. G. *Nat. Nanotechnol.* **2008**, *3*, 101–105.
- (9) (a) Gilje, S.; Han, S.; Wang, M.; Wang, K. L.; Kaner, R. B. *Nano Lett.* **2007**, *7*, 3394–3398. (b) Gómez-Navarro, C.; Weitz, R. T.; Bittner, A. M.; Scolari, M.; Mews, A.; Burghard, M.; Kern, K. *Nano Lett.* **2007**, *7*, 3499–3503. (c) Becerril, H. A.; Mao, J.; Liu, Z.; Stoltenberg, R. M.; Bao, Z.; Chen, Y. *ACS Nano* **2008**, *2*, 463–470. (d) Liu, P.; Gong, K. *Carbon* **1999**, *37*, 706–707.
- (10) (a) Geim, A. K.; Novoselov, K. S. *Nat. Mater.* **2007**, *6*, 183–191. (b) Novoselov, K. S.; A, K.; Geim, A. K.; Morozov, S. V.; Jiang, D.; Zhang, Y.; Dubonos, S. V.; Grigorieva, I. V.; Firsov, A. A. *Science* **2004**, *306*, 666–669. (c) Novoselov, K. S.; Jiang, D.; Schedin, F.; Booth, T. J.; Khotkevich, V. V.; Morozov, S. V.; Geim, A. K. *Proc. Natl. Acad. Sci.* **2005**, *102*, 10451–10453.
- (11) (a) Chen, G.; Wu, D.; Weng, W.; Wu, C. *Carbon* **2003**, *41*, 619–621. (b) Viculis, L. M.; Mack, J. J.; Mayer, O. M.; Hahn, H. T.; Kaner, R. B. *J. Mater. Chem.* **2005**, *15*, 974–978. (c) Chung, D. D. L. *J. Mater. Sci.* **2002**, *37*, 1475–1489.
- (12) (a) Watcharotone, S.; Dikin, D. A.; Stankovich, S.; Piner, R.; Jung, I.; Dommett, G. H. B.; Evmenenko, G.; Wu, S.; Chen, S.; Liu, C.; Nguyen, S. T.; Ruoff, R. S. *Nano Lett.* **2007**, *7*, 1888–1892. (b) Ruoff, R. *Nat. Nanotechnol.* **2008**, *3*, 10–11.

**Scheme 1.** Starting with SDBS-Wrapped GO, Reduction, and Functionalization of Intermediate SDBS-Wrapped CCG with Diazonium Salts



Similarly, GO dispersed in ceramic precursors and subsequently thermally treated yielded composites that imparted conductivity to an otherwise nonconductive matrix.<sup>12a</sup>

Previous work in our group has shown that aryl diazonium treatment of single-wall carbon nanotubes (SWCNTs)<sup>16</sup> produces functionalized SWCNTs; the diazonium chemistry gives us the capability of tailoring the functionalized materials by changing the addends. Functionalized SWCNTs have been shown to improve the dispersion and interfacial adhesion of the nanoreinforcing agent within the host matrix.<sup>17</sup> Likewise, substituted aryl groups can be readily anchored to other carbon surfaces such as graphite and glassy carbon by electrochemical reduction of diazonium salts.<sup>18</sup>

Here we report a convenient method to attain functionalized CCG (f-CCG) by reduction of GO with hydrazine followed by treatment with aryl diazonium salts. Although stable aqueous dispersions of CCG have been reported,<sup>5a,8,19</sup> direct use of CCGs is somewhat challenging because of the difficulty of redispersing the products in solvents after workup and recovery, unless stabilized by surfactants or molecules that prevent reaggregation.

## Experimental Section

**Graphite Oxide.** Graphite oxide was synthesized from expanded graphite obtained from SupraCarbonics, LLC using the

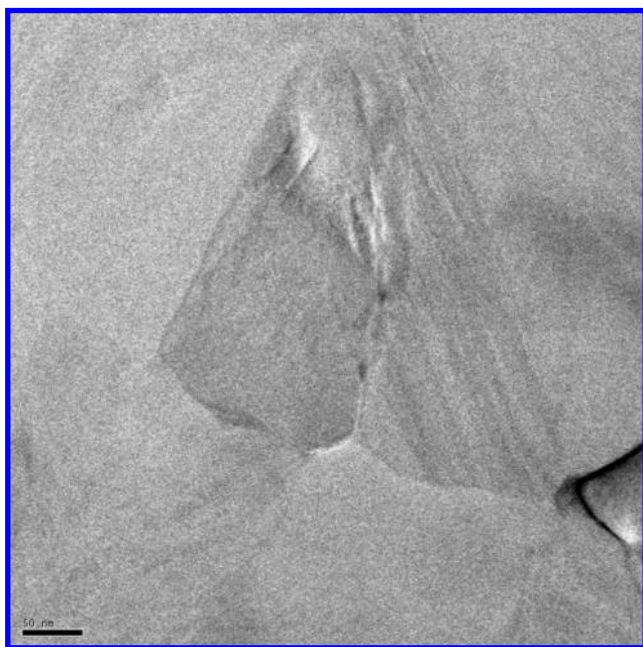


**Figure 1.** Cryo-TEM image of S-CCG. Scale bar is 50 nm.

Staudenmaier procedure.<sup>1b,6a</sup> Briefly, 5 g (416.7 mmol C) of expanded graphite was added in five portions to a stirred mixture of concentrated  $\text{H}_2\text{SO}_4$  (87.5 mL) and fuming  $\text{HNO}_3$  (45 mL) while cooling in an ice–water bath. To the mixture was added  $\text{KClO}_3$  (55 g) in five separate portions for a period of 15 min with sufficient venting using nitrogen gas to reduce the risk of explosion upon generation of chlorine dioxide gas. [Caution: protective equipment including face shield, acid-resistant gloves, and blast shield must be used at all times.] The resulting slurry was stirred at room temperature for 96 h. The green slurry was poured into 4 L of ice water, and the mixture was filtered and subsequently washed with 5 L of 5% HCl. The filter cake was then rinsed thoroughly with water until the filtrate was neutral. This was followed by rinsing the filter cake with methanol and diethyl ether, yielding 4.1 g of a fine brown powder of GO.

**Diazonium Functionalization.** The surfactant-wrapped dispersion of CCG (S-CCG) sheets was attained based on a similar procedure reported for SWCNT decant preparation.<sup>5a,20</sup> GO (225 mg) was dispersed in 1 wt % aqueous sodium dodecylbenzenesulfonate (SDBS) surfactant (225 mL) and homogenized for 1 h using a Dremel tool (400 xpr) fitted with a standard-capacity rotor-stator generator (Cole-Parmer A-36904-52) followed by cup horn sonication (Cole-Parmer Ultrasonic Processor model

- (13) (a) Niyogi, S.; Bekyarova, E.; Itkis, M. E.; McWilliams, J. L.; Hamon, M. A.; Haddon, R. C. *J. Am. Chem. Soc.* **2006**, *128*, 7720–7721. (b) Dekany, I.; Kruger Grasser, R.; Weiss, A. *Colloid Polym. Sci.* **1998**, *276*, 570–576.
- (14) (a) Matsuo, Y.; Nishino, Y.; Fukutsuka, T.; Sugie, Y. *Carbon* **2007**, *45*, 1384–1390. (b) Matsuo, Y.; Fukunaga, T.; Fukutsuka, T.; Sugie, Y. *Carbon* **2004**, *42*, 2117–2119. (c) Matsuo, Y.; Tabata, T.; Fukunaga, T.; Fukutsuka, T.; Sugie, Y. *Carbon* **2005**, *43*, 2875–2882.
- (15) Kotov, N. A.; Dekany, I.; Fendler, J. H. *Adv. Mater.* **1996**, *8*, 637–641.
- (16) (a) Bahr, J. L.; Yang, J.; Kosynkin, D. V.; Bronikowski, M. J.; Smalley, R. E.; Tour, J. M. *J. Am. Chem. Soc.* **2001**, *123*, 6536. (b) Bahr, J. L.; Tour, J. M. *Chem. Mater.* **2001**, *13*, 3823–3824. (c) Dyke, C. A.; Tour, J. M. *Nano Lett.* **2003**, *9*, 1215–1218. (d) Dyke, C. A.; Stewart, M. P.; Maya, F.; Tour, J. M. *Synlett.* **2004**, 155–160. (e) Doyle, C. D.; Rocha, J.-D. R.; Weisman, R. B.; Tour, J. M. *J. Am. Chem. Soc.* **2008**, *130*, 6795–6800. (f) Price, B. K.; Tour, J. M. *J. Am. Chem. Soc.* **2006**, *128*, 12899–12904.
- (17) (a) Mitchell, C. A.; Bahr, J. L.; Arepalli, S.; Tour, J. M.; Krishnamoorti, R. *Macromolecules* **2002**, *35*, 8825–8830. (b) Frankland, S. J. V.; Caglar, A.; Brenner, D. W.; Griebel, M. *J. Phys. Chem. B* **2002**, *106*, 3046–3048.
- (18) (a) Kariuki, J. K.; McDermott, M. T. *Langmuir* **2001**, *17*, 5947–5951. (b) Pan, Q.; Wang, H.; Jiang, Y. *J. Mater. Chem.* **2007**, *17*, 329–334. (c) Harnisch, J. A.; Gazda, D. B.; Andereg, J. W.; Porter, M. D. *Anal. Chem.* **2001**, *73*, 3954–3959. (d) Kariuki, J. K.; McDermott, M. T. *Langmuir* **1999**, *15*, 6534–6540. (e) Allongue, P.; Delamar, M.; Desbat, B.; Fagebaume, O.; Hitmi, R.; Pinson, J.; Saveant, J.-M. *J. Am. Chem. Soc.* **1997**, *119*, 201–207. (f) Delamar, M.; Hitmi, R.; Pinson, J.; Saveant, J. M. *J. Am. Chem. Soc.* **1992**, *114*, 5883–5884.
- (19) Si, Y.; Samulski, E. T. *Nano Lett.* **2008**, *8*, 1679–1682. At the time of revising this manuscript, this research was published.
- (20) Moore, V. C.; Strano, M. S.; Haroz, E.; Hauge, R. H.; Smalley, R. E. *Nano Lett.* **2003**, *7*, 1379–1382.

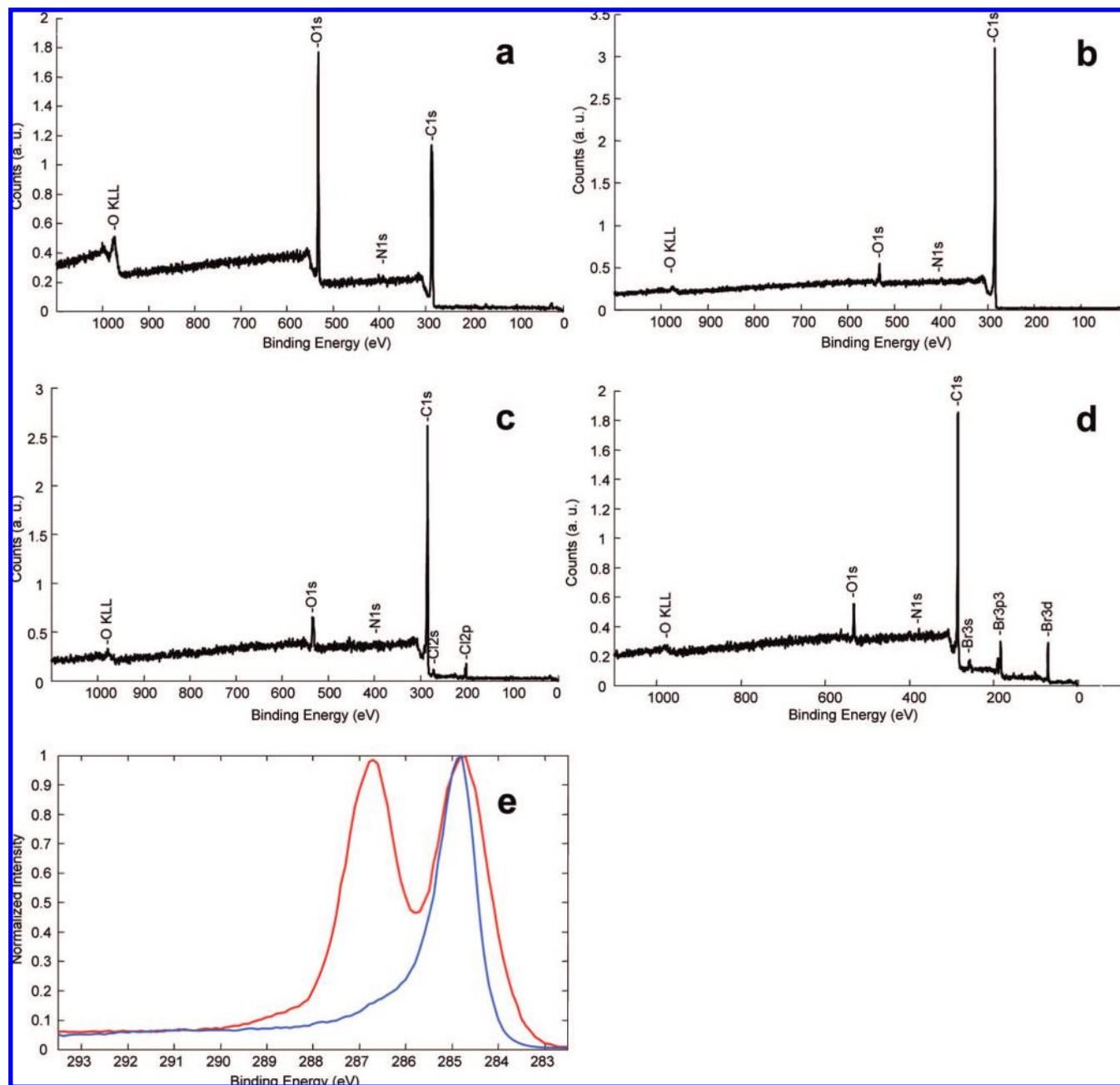


**Figure 2.** XPS Survey scan of (a) GO, (b) S-CCG, (c) **1b**, and (d) **4b**. (e) High-resolution XPS C1s spectra of GO (red) and S-CCG (blue) showing significant loss of C–O and C=O groups after reduction. XPS was carried out on a PHI Quantera SXM Scanning X-ray Microprobe with a base pressure of  $5 \times 10^{-9}$  Torr, with an Al cathode as the X-ray source set at 100 W and a pass energy of 140.00 (survey scan) and 26.00 eV (high-resolution scan),  $45^\circ$  takeoff angle, and a  $100 \mu\text{m}$  beam size.

CP 750) at 80% power for 10 min. The pH was adjusted to 10 (measured with pH paper) using 1 M aqueous NaOH. The resulting GO dispersion was reduced with 60% hydrazine hydrate (2.25 mL, 72.23 mmol) at  $80^\circ\text{C}$  for 24 h<sup>5a</sup> followed by filtration using glass wool to remove large aggregates, yielding the S-CCG dispersion decant with a typical concentration of 1 mg/mL. In a typical functionalization procedure (Scheme 1) 20 mL of S-CCG dispersion was reacted with an aryl diazonium salt (0.33 mmol/mL S-CCG) for 1 h at room temperature. The mixture was then diluted with 100 mL of acetone and filtered through a  $0.45 \mu\text{m}$  PTFE (Teflon) membrane. The filter cake was washed with water and acetone ( $3 \times$ ) and resuspended in DMF to remove SDBS and excess diazonium salt. This was followed by filtration ( $0.45 \mu\text{m}$  PTFE) and copiously washing the filter cake with acetone.

The resulting solid was dried in a vacuum oven overnight at  $70^\circ\text{C}$  with a yield of 22–24 mg of f-CCG.

## Results and Discussion

Owing to the high yield of individual sheets, chemical oxidation of graphite to GO is one of the preferred methods to achieve nanosheets from graphite. For preparation of composites where large quantities are required, mechanical cleavage is less attractive.<sup>12b</sup> Use of reducing agents such as hydroquinone,  $\text{NaBH}_4$ , and hydrazine have all been shown to be effective in removing most of the oxygen-containing groups<sup>2,3d–e,5</sup> and to a certain extent restore the conductivity of the material, albeit several orders of magnitude lower (in



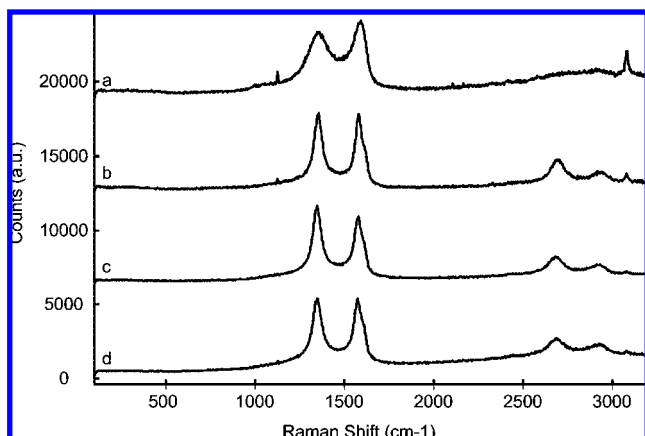


**Figure 3.** Raman spectra of (a) GO, (b) S-CCG, (c) **1b**, and (d) **1b** after heating under Ar to 850 °C.

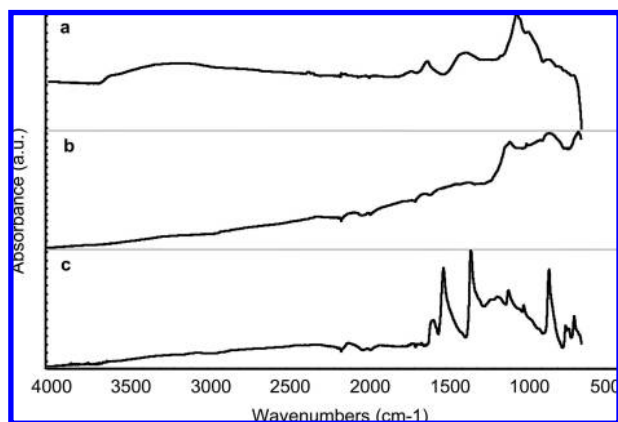


**Figure 4.** ATR-IR spectra of (a) GO, (b) S-CCG, and (c) f-CCG **2b**.

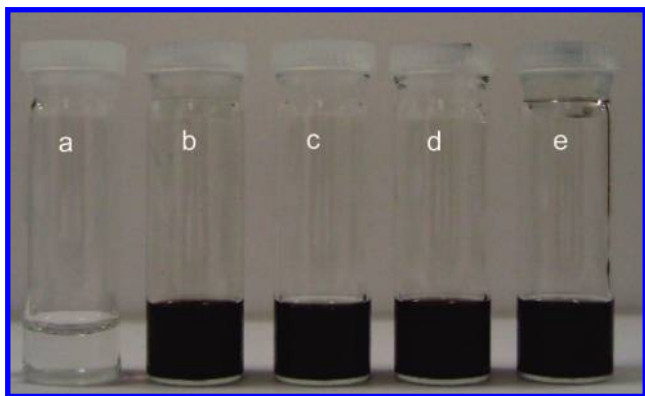


**Figure 5.** Photographs of supernatant DMF solutions obtained from dispersions of (a) CCG and (b) **4b**, (c) **1b**, (d) **2b**, and (e) **3b** after centrifugation for 15 min at 3200 rpm.

$\Omega \text{ cm}^{-1}$ ) than that of graphene.<sup>11</sup> In situ reductions within matrices have also been shown to render the composites conductive.<sup>12</sup>

Prior to functionalization the S-CCG sheets were analyzed in their solution environments by cryogenic transmission electron microscopy (cryo-TEM) to establish the existence of individual sheets and a few multiple sheet structures (Figure 1). Aqueous CCG dispersions without SDBS were also prepared based on the procedure reported by Li et al.,<sup>8</sup> treated with aryl diazonium salts, and found to react similarly

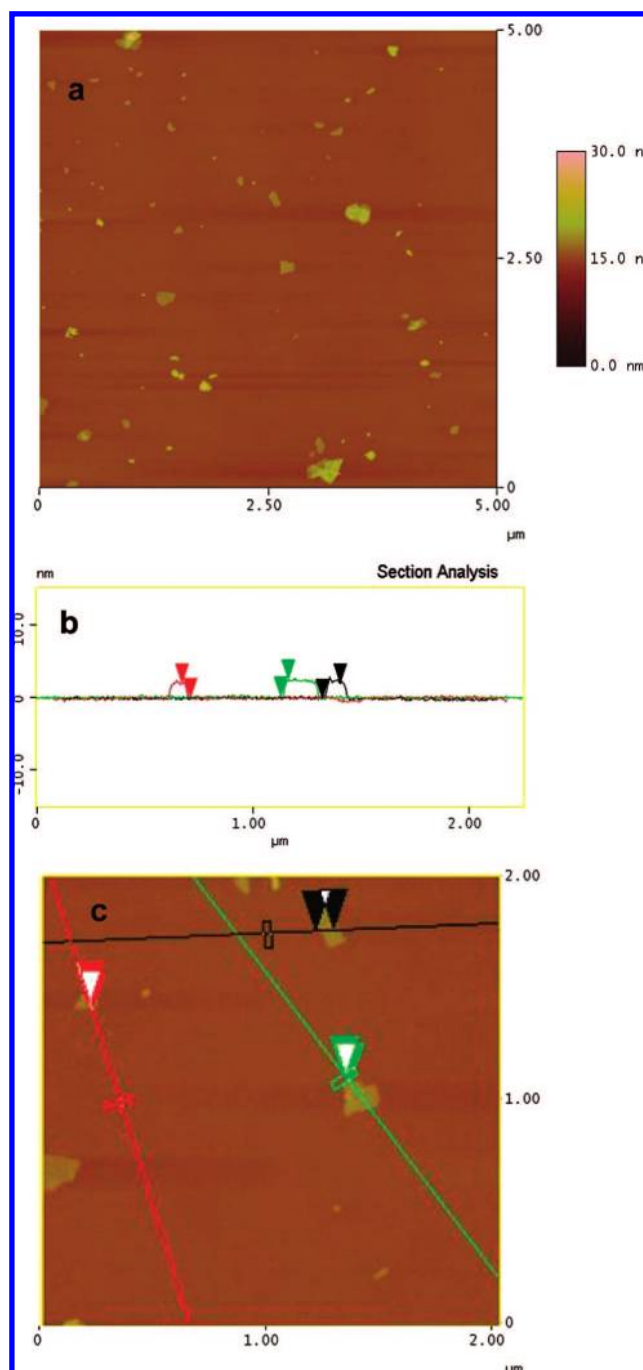


**Figure 6.** (a) Atomic force micrographs by height of f-CCG **2b** spin coated onto a freshly cleaved mica surface showing single f-CCG sheets accompanied by bilayers to several layers. (b) Section analysis of **2b** showing height ranges from 1.8 to 2.2 nm (red, green, and black lines) for the imaged regions shown in c.

in conjunction with the findings of Si et al.<sup>19</sup> However, diazonium functionalization is maximized with the use of S-CCG decants due to a more concentrated nanosheet dispersion (1 mg/mL based on GO weight) compared to the nanosheets from aqueous CCG (0.25 mg/mL).

Removal of a majority of the oxygen groups by hydrazine has been verified using X-ray photoelectron spectroscopy (XPS) as reported by several groups.<sup>5a,6,9b,c</sup> The C1s spectrum of the CCG shows a significant decrease of signals at 286–288 eV, which indicates loss of C–O and C=O

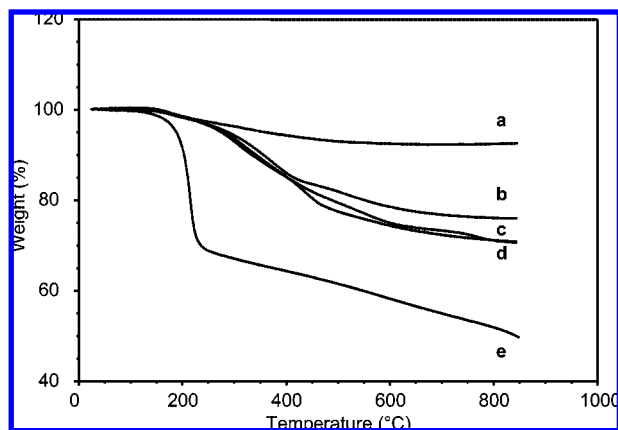


**Figure 7.** TGA thermograms of (a) CCG, (b) **2b**, (c) **3b**, (d) **1b**, and (e) GO.

functionalities (Figure 2). The surface oxygen groups in GO were estimated to be 32% with little nitrogen (0.4%), while after treatment with hydrazine the percentage of oxygen decreased to 8.7% with 1.4% nitrogen. The small increases of nitrogen content can be attributed to hydrazones.<sup>5a,9c</sup> Upon treatment with the diazonium salts a significant percentage of halogen markers, Cl or Br, was detected with very little accompanying nitrogen, which implies that the surface has been successfully functionalized. High-resolution XPS of **1b** and **4b** gave the following atomic percentages of halogens: (**1b**) 4.6% Cl and (**4b**) 3.2% Br with  $\sim 1\%$  N (see Supporting Information). A control experiment was conducted by adding chlorobenzene to the S-CCG decant followed by workup and XPS analysis to rule out the possibility that Cl was present due to physisorption and intercalation of chlorinated materials between the sheets. XPS analysis showed no Cl peak at 200 eV. Furthermore, GO without hydrazine reduction and treated with **4a** showed no Br peak after workup. Hence, successful functionalization supports the assumption that partial rearomatization of the nanosheets under the hydrazine reduction conditions has occurred and thereby provided a surface for aryl grafting using the diazonium species.<sup>19</sup>

The Raman spectrum of bulk CCG using 514 nm laser excitation shows a similar profile to that of GO with a diamondoid (D) to graphitic (G) ratio close to 1, confirming incomplete recovery of graphene structure, similar to what was observed for thermally reduced graphene.<sup>5,6</sup> However, the 2D peak at  $\sim 2700$  is more pronounced on reduced samples compared to the parent GO, which is an indication of the  $sp^2$  network being present within the sheets. After functionalization with diazonium salts as described here the D to G ratios of the f-CCGs were similar to those of the S-CCG; therefore, gauging the degree of functionalization was difficult using Raman spectroscopy. f-CCG samples heated in a thermogravimetric analysis (TGA) instrument to 850 °C under argon also showed some decrease in the intensity of the diamondoid peak, consistent with defunctionalization upon heating (Figure 3). Edge defects may be responsible for the minimal change in the D/G ratios, although larger CCG sheets ( $\sim 2 \mu\text{m}$ ) evaluated by Raman also gave the same profile.<sup>9b</sup>

The IR spectrum (Figure 4a) of GO shows a C–O stretch at  $\sim 1200 \text{ cm}^{-1}$  and O–H stretch at  $3500\text{--}3300 \text{ cm}^{-1}$  as well as a C=O stretch at  $1720\text{--}1690 \text{ cm}^{-1}$ . The S-CCG (Figure 4b), however, is devoid of any informative signal and

resembles that of bulk graphite. Figure 4c shows the ATR-IR spectrum of f-CCG **2b**. Asymmetric and symmetric stretches at  $1513$  and  $1343 \text{ cm}^{-1}$ , respectively, are attributed to the  $\text{NO}_2$  group and the C–N stretch at  $852 \text{ cm}^{-1}$ , and the aromatic stretch at  $1586 \text{ cm}^{-1}$  indicates the presence of nitrobenzene moieties on the f-CCG sheets.<sup>18e,f</sup> The presence of  $\text{NO}_2$  was further confirmed by XPS with a strong signal at 406 eV (see Supporting Information). Also, the absence of azo groups in the  $1400\text{--}1500 \text{ cm}^{-1}$  region in the spectra of the halogen-containing f-CCGs supports the assumption that a radical process is operating in the functionalization with diazonium salts, similar to the process with SWCNTs, thereby generating the aryl radicals.<sup>16c–e</sup>

The f-CCGs can be readily dispersed in *N,N'*-dimethylformamide (DMF), *N,N'*-dimethylacetamide (DMAc), and 1-methyl-2-pyrrolidinone (NMP) up to 1 mg/mL with minimal sedimentation (Figure 5). To further illustrate their respective solubilities in DMF, 3 mg of S-CCG or f-CCGs was dispersed in 3 mL of DMF using an ultrasonic cleaner (Cole-Parmer model 08849-00) for 5 min followed by centrifugation in an Adams Analytical centrifuge (model CT 3201) for 15 min at 3200 rpm, after which a 2 mL aliquot of each supernatant (Figure 5) was taken and precipitated in acetone and filtered, and the filter cake was washed with acetone, dried, and weighed. The supernatant of f-CCGs gave dark solutions with some sedimentation, while nothing remained in the S-CCG supernatant; everything settled to the bottom, and hence, the solubility is taken as near zero. The solubilities of the f-CCGs are as follows: **1b**, 0.25 mg/mL; **2b**, 0.45 mg/mL; **3b**, 0.30 mg/mL; and **4b**, 0.50 mg/mL.

Individual functionalized graphene sheets were imaged using tapping mode AFM. Figure 6 shows images of graphene sheets spin coated onto a mica surface using a 0.1 mg/mL dispersion of **2b** in DMF. The theoretical height for a graphene sheet functionalized on both sides is  $\sim 2.2$  nm, assuming that the height of the bare graphene sheets is 1 nm<sup>5a,9b,c</sup> with the substituted aromatic groups contributing  $\sim 0.6$  nm in heights. On average, the height of f-CCG sheets ranges from 1.8 to 2.2 nm. Overall, the nanosheets may be composed of single or bilayers of graphene sheets.

The presence of functional groups on the graphene sheets was further analyzed using TGA by heating under an argon atmosphere to 850 °C at a rate of  $10 \text{ }^\circ\text{C}/\text{min}$  (Figure 7).<sup>16c,e</sup> The overall weight loss of S-CCG is  $\sim 7.4\%$ , which can be attributed mostly to the COOH groups that are not reduced by hydrazine treatment as well as incomplete rearomatization. On the other hand, heating GO produced a weight loss of 50%. The observed weight loss for the f-CCG sheets are as follows: **1b**, 29%; **2b**, 24%; **3b**, 29%; **4b**, 31%. The degree of functionalization is estimated to be  $\sim 1$  functional group in 55 carbons from these weight losses. This underscores the efficacy of the functionalization method described here.

## Conclusion

We employed a convenient procedure, originally developed for functionalization of SCWNTs, to functionalize CCGs with high amounts of varying aryl addends, allowing these nanosheets to be solubilized in organic solvents. This development may prove to be useful in the area of composites, especially in the use of these 2-D structures as reinforcing agents where intimate interfacial bonding between the host and the structural modifier is critical. Unlike the

1-D-functionalized SWCNT composites, these 2-D structures should be of particular interest where gas diffusion or separation barriers are sought from the composite frameworks.

**Acknowledgment.** We thank AFOSR/AFRL, NASANNX07AI65G, and the Federal Aviation Administration 2007G010 for financial support and Dr. Wenhua Guo for the cryo-TEM imaging.

**Supporting Information Available:** AFM micrograph of S-CCG and XPS spectra of **1b**, **2b**, and **4b**. This material is available free of charge via the Internet at <http://pubs.acs.org>.

JA806499W